MBene Promoted Zn Peroxide Chemistry for Rechargeable Near-Neutral Zn-Air Batteries

*Yue Hou[1], Ze Chen[1], Xinliang Li[5], Yiqiao Wang[1], Pei Li[1], Huilin Cui[1], Rong Zhang[1], Shuo Yang[1], Shaoce Zhang[1], Chunyi Zhi[1,2,3,4]**

[1]Department of Materials Science and Engineering, City University of Hong Kong, 83 Tat Chee Avenue, Kowloon, Hong Kong 999077, China

[2]Hong Kong Institute for Advanced Study, City University of Hong Kong, Kowloon, Hong Kong, 999077, China

[3]Hong Kong Institute for Clean Energy, City University of Hong Kong, Kowloon 999077, Hong Kong

[4]Centre for Functional Photonics, City University of Hong Kong, Kowloon, Hong Kong.

[5]Key Laboratory of Material Physics, Ministry of Education, School of Physics and Microelectronics, Zhengzhou University, Zhengzhou 450001, China

*E-mail: cy.zhi@cityu.edu.hk

Experimental

1. Materials Preparation

Synthesis of $Mo_{2/3}B_{1/2}T_z$ MBene: The three-dimensional (3D) $Mo_{2/3}Y_{1/3}AlB_2$ *i*-MAB phase was purchased from the Beijing Beike New Material Technology Co., Ltd. 1 g of the *i*-MAB precursor was slowly etched by 10 ml 40 wt% aqueous hydrofluoric (HF) acid at room temperature, and then the above solution was stirred in an oil bath maintaining a temperature of 35 °C for about 3.5 h. After etching, the slurry was diluted and washed with deionized water three times to eliminate the reaction products. For further delamination, the above solution was transferred to a beaker in an ice bath and sonicated by a cell crusher for 5 h. The cell crusher was carried out in the intermittent mode with pulse on 1s and pulse off 1s. The whole processing time is 1 hour. And the ultrasound was carried out in mono-frequency mode (20 kHz) with a Φ6 mm luffing rod. Finally, the few-layer MBene powder can be obtained by freeze-drying the

previous supernatant solution in a lyophilizer for 48 h.

MBene coated on carbon cloth (MBene): For fabrication of the MBene cathode, 5 mg MBene, 1 mg conductive carbon black, and 50 μL of a 5 wt% Nafion solution were dispersed into 1 mL solution (the volume of isopropanol: water = 1:1), and then under sonication for 30 minutes. Next, the homogenous dispersion was dropped onto the cleaned carbon cloth using a doctor-blading method. The slurry was then dried in a vacuum oven setting at 80 ℃ for 12 h to remove the isopropanol. The mass of the MBene catalyst was controlled to achieve a mass loading amount of 1.0 mg cm^{-2}.

PtC+IrO_2 coated on carbon cloth (PtC+IrO_2): The catalyst ink was prepared by blending 5 mg PtC+IrO_2 and 50 μL of a 5 wt% Nafion solution into1 mL solution (the volume of isopropanol: water = 1:1) under sonication for 30 minutes. The dispersion was transferred onto the cleaned carbon cloth via a controlled drop-casting method. The slurry was then dried in a vacuum oven setting at 80 ℃ for 12 h to remove the isopropanol. The mass of the Pt/C+IrO_2 was controlled to obtain a loading amount of 1.0 mg cm^{-2}.

Ketjen black coated on carbon cloth (Ketjen black): The catalyst ink was prepared by blending 5 mg conductive ketjen black and 50 μL of a 5 wt% Nafion solution into 1 mL solution (the volume of isopropanol: water = 1:1) under sonication for 30 minutes. The dispersion was transferred onto the cleaned carbon cloth via a controlled drop-casting method. The slurry was then dried in a vacuum oven setting at 80 ℃ for 12 h to remove the isopropanol. The mass of ketjen black was controlled to obtain a loading amount of 1.0 mg cm^{-2}.

Synthesis of polyacrylamide (PAM) hydrogel electrolyte

The PAM hydrogel with zinc trifluoromethanesulfonate ($Zn(OTf)_2$) is employed as the quasi-solid electrolyte to fabricate the ZAB-MBene pouch cell. Firstly, 0.1 mol $Zn(OTf)_2$ is dissolved into 100 ml DI water. Then, we added 10 g acrylamide monomer into the above solution with a stirring treatment at 40 °C. The above solution is added by cross-linkers (2 mg N, N'-methylenebisacrylamide) and initiator (50 mg potassium persulfate) with heat preservation of 40 °C for 2 hours. Then the mixture is degassed under a nitrogen atmosphere to avoid the negative effect of remaining oxygen on the

free-radical polymerization. In the last step, the PAM hydrogel electrolyte is obtained after 40 °C heat treatment for 2 hours.

Materials characterization

X-ray diffraction (XRD) patterns of the samples were carried out in an X-ray diffractometer equipment (XRD; Bruker, D2 Advance) with Cu Ka radiation. The microstructure and chemical composition were detected by a field emission scanning electron microscopy, SEM (S-4700, Hitachi) with an energy dispersive spectrometer (EDS), transmission electron microscopy (TEM; FEI Tecnai F20), and scanning transmission electron microscope (STEM) combined with high angle-annular dark-field (STEM-HAADF; Titan Cubed Themis G2300, 300 kV) imaging, and electron energy loss spectroscopy (EELS) analysis. Nitrogen gas sorption measurements at 77 K were carried out with an automatic system (ASAP2460, Micromeritics Inc., USA). The samples were outgassed under vacuum conditions at 473 K for 3 h before test. Brunauere-Emmette-Teller (BET) method was used to calculate the BET-specific surface area (BET-SSA) in the linear relative pressure range of 0.0-1.0. X-ray photoelectron spectroscopy (XPS; ESCALAB 250) is employed to analyze the surface composition details with C 1s peak calibration at 284.8 eV. XPS spectra were recorded for O 1s, Mo 3d, Zn 2p, and B 1s. The discharged/charged air cathodes and Zn anodes were gently washed with deionized water three times and then dried at room temperature for 24h before measurements.

Electrochemical measurements

The CR2032 coin-type cell was assembled to measure the electrochemical performances of the ZAB with different samples. A multichannel electrochemical workstation of CHI 760D was employed to carry out cyclic voltammetry (CV) and electrochemical impedance spectroscopy (EIS) results. The frequency of EIS ranges from 10^5 to 0.1 Hz. The cyclic performances, rate performances, and gravimetric capacity of the ZAB assembled with different active materials were tested on a LAND CT3001A battery testing device. The zinc metal foil is directly used as the anode and separated from the above cathode by commercial glass fiber to fabricate the final zinc-air cells. The thickness of Zn foil is 80 μm, and the separator type is the Whatman glass

fiber 260 μm. The electrolyte for this cell is 1M $Zn(OTf)_2$, prepared by dissolving 0.1 mol $Zn(OTf)_2$ into 100 ml DI water. 100 μL electrolytes (1m $Zn(OTf)_2$) have been added for each coin-cell NNZAB, which makes sure the full immersion of the glass fiber separator to keep good contact between the electrolyte-electrode interface. All electrochemical performances were calculated based on the mass of catalysts.

DFT Calculations

The first principles calculation in this work was conducted using the Castep code in the Materials Studio software based on density functional theory (DFT), in which the projector augmented wave (PAW) pseudopotentials are selected to analyze the ion-electron interactions.[1, 23] The generalized gradient approximation in the Perdew-Burke-Ernzerhof (GGA-PBE) form was selected to treat the exchange-correlation functional. The cutoff energy for the plane-wave basis set was set as 489.80 eV. The model of $Mo_{4/3}Y_{2/3}AlB_2$ was constructed with a hexagonal symmetry and a space group of R-3M (#166) (the lattice parameter of a = b = 5.44577 Å and c = 22.69048 Å). The model of $Mo_{4/3}B_2$ was built by removing the Y and Al atoms due to the etching. A 3×3×1 supercell of $Mo_{4/3}B_2$ was employed, and a gamma-centered 3×3×1 Monkhorst-Pack k-point mesh was set as the Brillouin zone. To achieve a reasonable structure, the convergence criterion of the total energy was set to be within 1×10^{-5} eV within the *k* points integration, and all the geometries were optimized until the maximum force was less than 0.02 eV $Å^{-1}$. We also constructed a vacuum space of 20 Å in z-direction to eliminate interactions between the considered phase and the closest layers.

The following formula guided the adsorption energy (E_{ads}):

$$E_{ads}=E_{all}-E_{MBene}-E_{ZnO_2}$$

in which E_{total}, E_{MBene}, and E_{ZnO_2} represent the energy of MBene nanosheets adsorbed with ZnO_2 molecules, pure MBene, and pure ZnO_2 molecules, respectively.

The reaction free energy of each reaction coordinate was calculated by the equation:

$$\Delta G = E - E_0 + \Delta n_{Zn} (\mu_{Zn} - eU) + \Delta n_O \mu_O, \quad (5)$$

E and E_0 represent the total energy of the system at specific and initial steps. Δn_{Zn} and Δn_O are the adsorbed/desorbed numbers of Zn and O_2 for each step. μ_{Zn} and μ_O are the

chemical potentials of Zn and O_2. U is the electromotive force corresponding to the discharging, equilibrium, and charging voltage.

The calculated overpotential of ORR and OER processes was defined as

$$\eta_{ORR/OER} = |U_{DC/C} - U_0|, \quad (6)$$

and total potential was

$$\eta_{TOT} = \eta_{ORR} + \eta_{OER}. \quad (7)$$

U_{DC} and U_C are the discharge and charge potential which drives all ORR or OER steps energetically downhill, respectively. U_0 is the equilibrium potential, making the ORR/OER process occur spontaneously ($\Delta G \leq 0$).

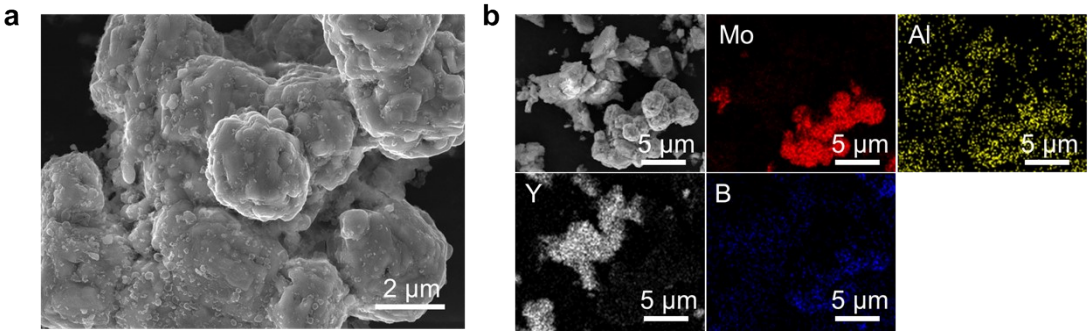

Figure S1. SEM image of the *i*-MAB phase $(Mo_{2/3}Y_{1/3})_2AlB_2$).

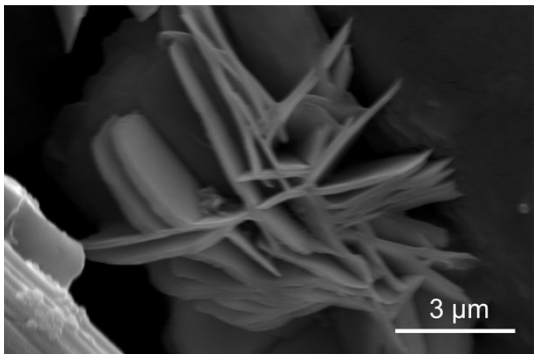

Figure S2. SEM image of the multilayer $Mo_{4/3}B_{2-x}T_z$ MBene.

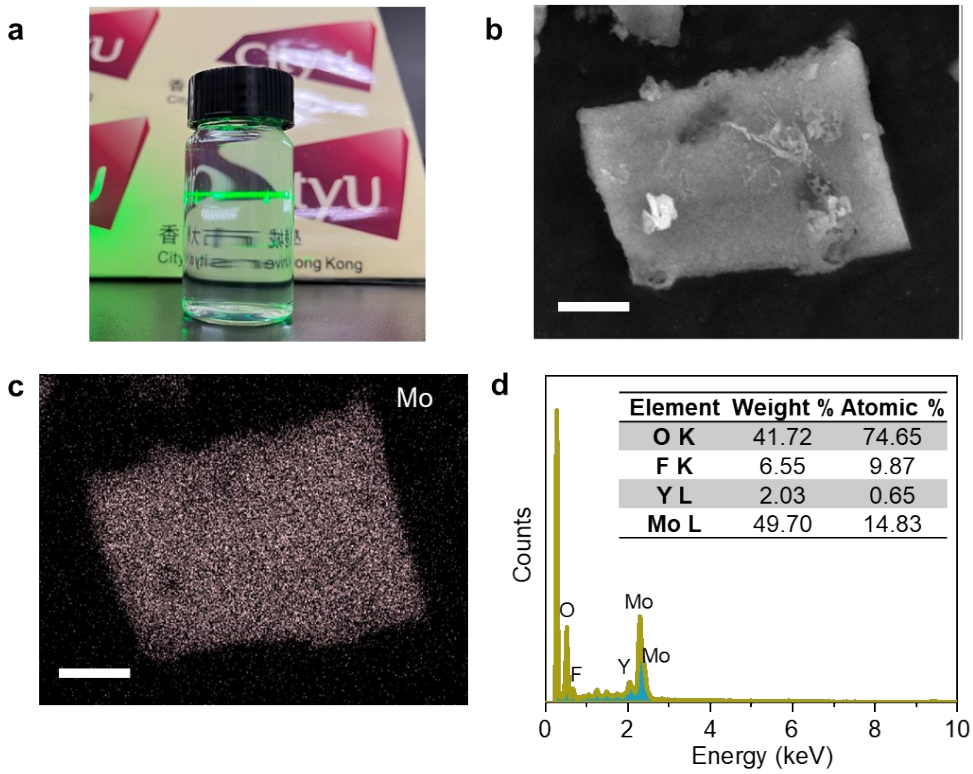

Figure S3. (a) Optical image of the Tyndall effect of $Mo_{4/3}B_{2-x}T_z$ MBene dispersed in water; SEM image **(b)** of the $Mo_{4/3}B_{2-x}T_z$ MBene with a corresponding EDS mapping pattern of Mo element **(c)** and the EDS data **(d)**. The scale bar in **(b)** and **(c)** is 2 μm.

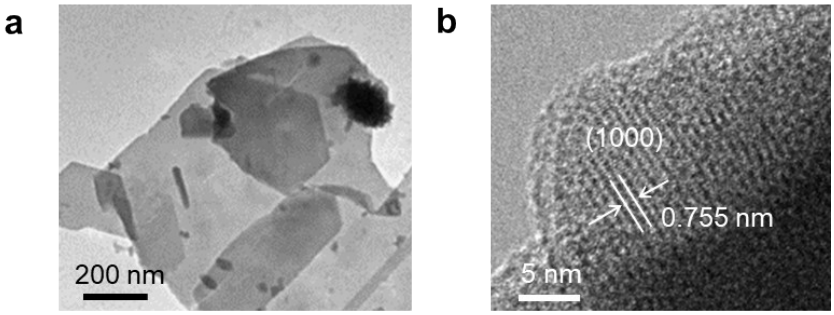

Figure S4. (a) TEM and **(b)** HRTEM image of the fabricated $Mo_{4/3}B_{2-x}T_z$ MBene.

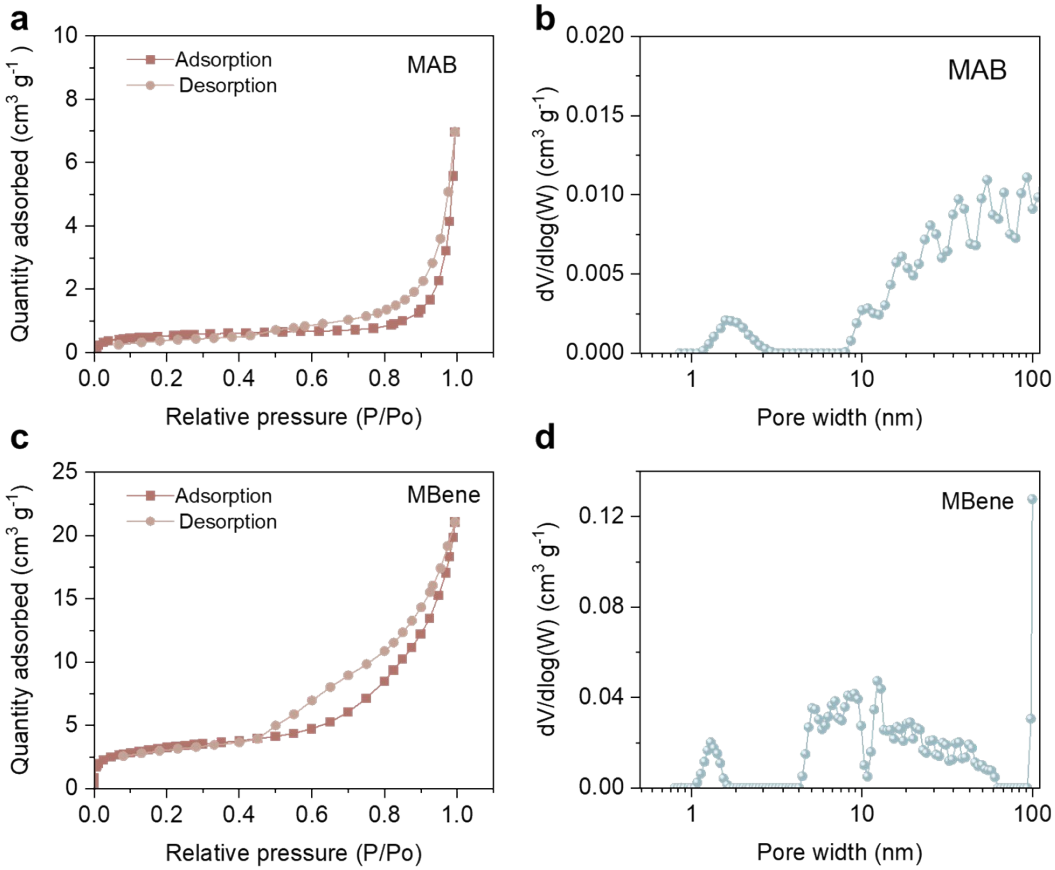

Figure S5. (a) Nitrogen adsorption/desorption isotherms and **(b)** pore size distribution of the *i*-MAB phase $(Mo_{2/3}Y_{1/3})_2AlB_2$). **(c)** Nitrogen adsorption/desorption isotherms and **(d)** pore size distribution of the fabricated $Mo_{4/3}B_{2-x}T_z$ MBene.

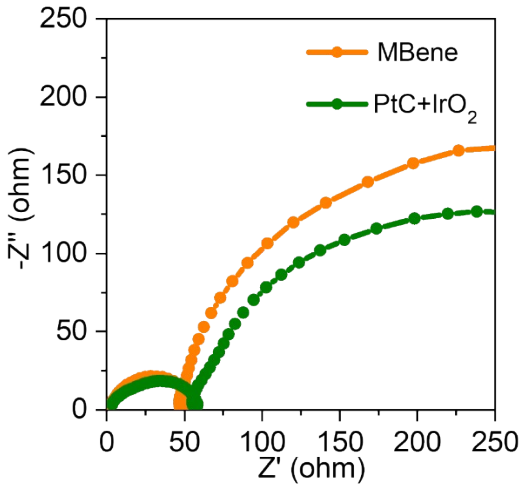

Figure S6. EIS pattern of the NNZAB-MBene and the NNZAB-PtC+IrO_2 at pristine

states.

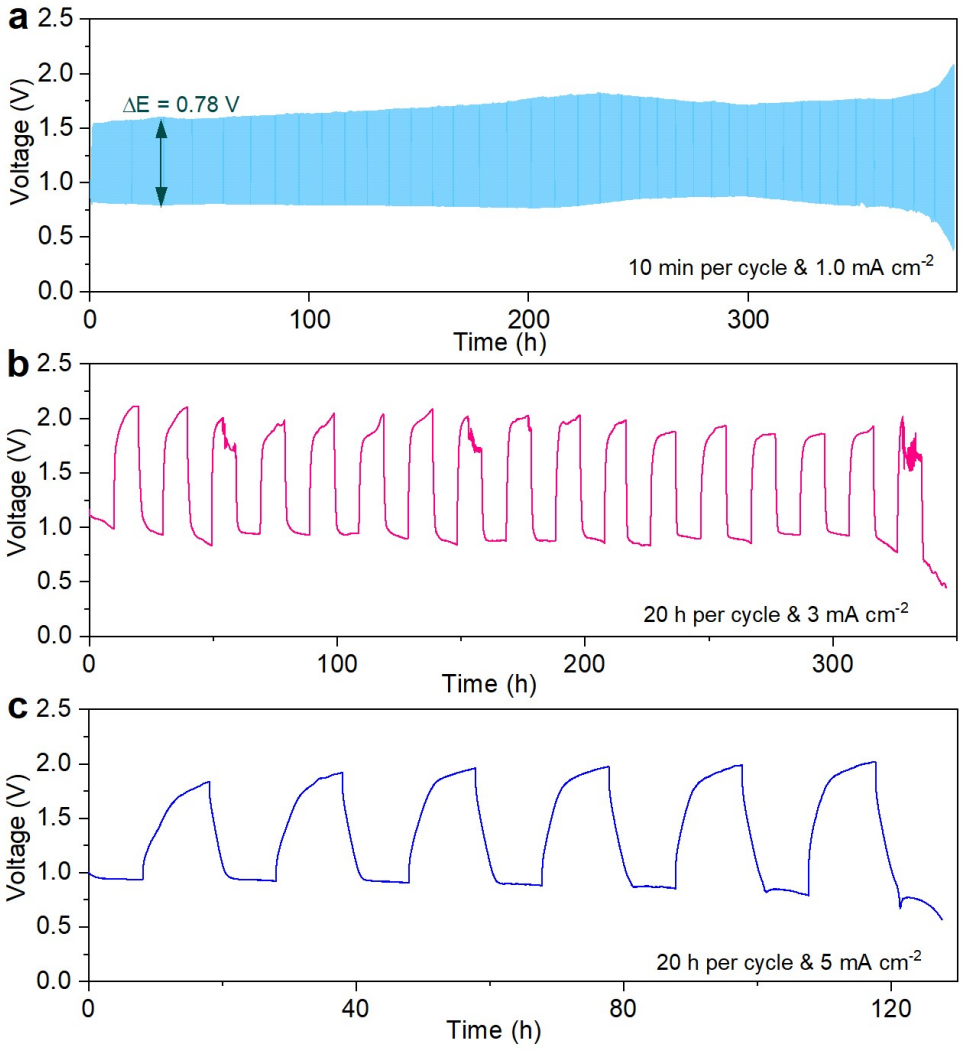

Figure S7. (a) The cycling performance of NNZAB-MBene at a current density of 1.0 mA cm^{-2} with a 10-min charge and discharge per cycle; **(b)** The cycling performance of NNZAB-MBene at a current density of 3.0 mA cm^{-2} with a 20-hour charge and discharge per cycle; **(c)** The cycling performance of NNZAB-MBene at a current density of 5.0 mA cm^{-2} with a 20-hour cycle period.

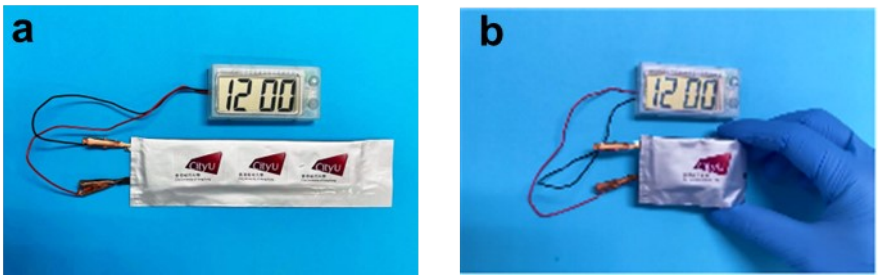

Figure S8. Demonstration of a NNZAB-MBene pouch cell powering an electric watch before **(a)** and after bending **(b)**.

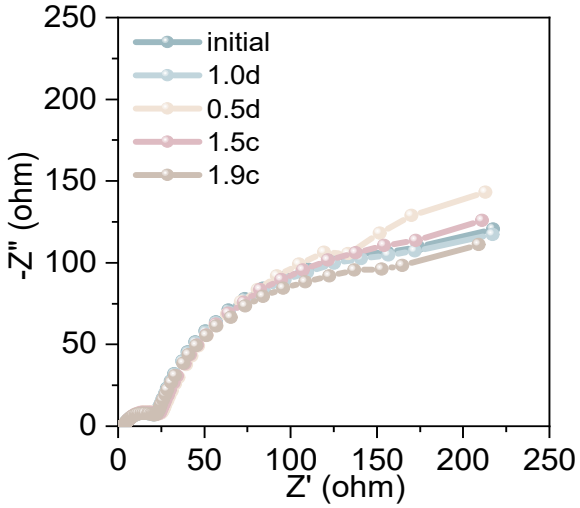

Figure S9. EIS pattern of the NNZAB-MBene obtained from the NNZABs at different discharge and charge states.

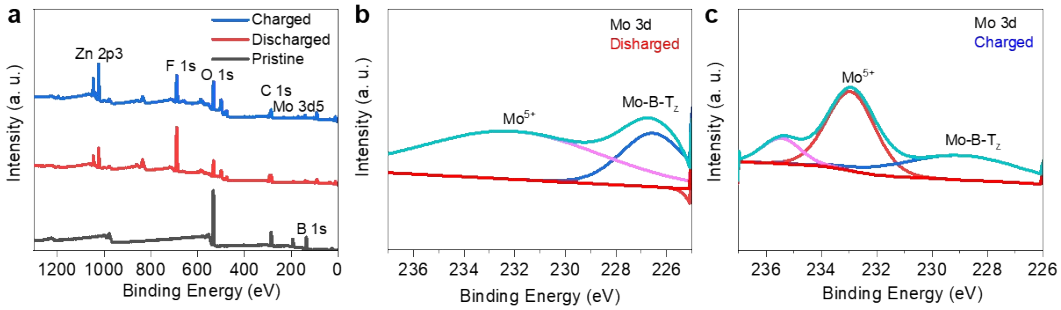

Figure S10. **(a)** XPS survey spectra of the $Mo_{4/3}B_{2-x}T_z$ MBene cathodes obtained from the NNZABs at pristine state, after the 1st discharged, and after 1st charged state; high-resolution XPS spectra of the Mo 3d for the $Mo_{4/3}B_{2-x}T_z$ MBene cathodes after the 1st discharged **(b)**, and after 1st charged **(c)** states.

Table S1. Cycle performances of this work, and reported other cathodes based on near neutral and alkaline electrolytes of ZABs.

Catalyst	**Electrolytes**	**Loading mass (mg cm)**	**Current (mA cm^{-2})**	**Cycle Time (h)**	**Ref.**
Co-NCNT	6.0 M KOH with 0.2 M $Zn(Ac)_2$	1	2 / 5	72/60	4
BFC	6.0 M KOH with 0.2 M $Zn(Ac)_2$	1	2	105	5
FeN_x-PNC	6.0 M KOH with 0.2 M $Zn(Ac)_2$	2	5	40	6
60% Pt+RuO_2	6.0 M KOH with 0.2 M $Zn(Ac)_2$	10	2	160	7
CoPOF@ CNT	6 M KOH	2.0	2	110	8
NiFe@C @Co CNF	6.0 M KOH with 0.2 M $Zn(Ac)_2$	0.5	2	320	9
CCNF-PDIL	6.0 M KOH with 0.2 M $Zn(Ac)_2$	0.5	2	240	10
NGM-Co	6.0 M KOH with 0.2 M $Zn(Ac)_2$	1.5	2	60	11
(Zn)Co-NCF	6.0 M KOH with 0.2 M $Zn(Ac)_2$	1	2	277	12
M–N–C	6 M KOH	0.5	5	81	13

Carbon black	1 M $Zn(OTf)_2$	8	0.4/1	300/160	14
This Work	**1 M $Zn(OTf)_2$**	**1**	**1/2/3/5**	**390/380/340/120**	**This work**

References

[1] X. Li, Q. Li, Y. Hou, Q. Yang, Z. Chen, Z. Huang, G. Liang, Y. Zhao, L. Ma, M. Li, Q. Huang, C. Zhi, *ACS nano* **2021**, 10.1021/acsnano.1c04354.

[2] S. Grimme, *Journal of computational chemistry* **2006**, *27*, 1787.

[3] K. B. John P. Perdew, Matthias Ernzerhof, *Physical Review Letters* **1996**, *77*, 3865.

[4] Z. Pei, Y. Huang, Z. Tang, L. Ma, Z. Liu, Q. Xue, Z. Wang, H. Li, Y. Chen, C. Zhi, *Energy Storage Materials* **2019**, *20*, 234.

[5] Z. Pei, Z. Yuan, C. Wang, S. Zhao, J. Fei, L. Wei, J. Chen, C. Wang, R. Qi, Z. Liu, Y. Chen, *Angew Chem Int Ed Engl* **2020**, *59*, 4793.

[6] L. Ma, S. Chen, Z. Pei, Y. Huang, G. Liang, F. Mo, Q. Yang, J. Su, Y. Gao, J. A. Zapien, C. Zhi, *ACS nano* **2018**, *12*, 1949.

[7] Y. Huang, Z. Li, Z. Pei, Z. Liu, H. Li, M. Zhu, J. Fan, Q. Dai, M. Zhang, L. Dai, C. Zhi, *Advanced Energy Materials* **2018**, *8*, 1802288.

[8] H. Zhang, Z. Qu, H. Tang, X. Wang, R. Koehler, M. Yu, C. Gerhard, Y. Yin, M. Zhu, K. Zhang, O. G. Schmidt, *ACS Energy Letters* **2021**, *6*, 2491.

[9] X. Chen, J. Pu, X. Hu, Y. Yao, Y. Dou, J. Jiang, W. Zhang, *Small* **2022**, *18*, e2200578.

[10] H. D. Mi Xu, Zhen Zhang, Yun Zheng, Bohua Ren, Qianyi Ma, Guobin Wen, Dan Luo, Aiping Yu, Luhong Zhang, Xin Wang, and Zhongwei Chen, *Angew. Chem. Int. Ed.* **2022**, *e202117703*, 1.

[11] C. Tang, B. Wang, H. F. Wang, Q. Zhang, *Advanced materials* **2017**, *29*,

[12] Y. Ma, D. Chen, W. Li, Y. Zheng, L. Wang, G. Shao, Q. Liu, W. Yang, *Energy & Environmental Materials* **2022**, *5*, 543.

[13] G. Yang, J. Zhu, P. Yuan, Y. Hu, G. Qu, B. A. Lu, X. Xue, H. Yin, W. Cheng, J. Cheng, W. Xu, J. Li, J. Hu, S. Mu, J. N. Zhang, *Nature communications* **2021**, *12*, 1734.

[14] F. W. Wei Sun, Bao Zhang, Mengyi Zhang, Verena Küpers, Xiao Ji, Claudia Theile, Peter Bieker, Kang Xu, Chunsheng Wang, Martin Winter, *Science* **2021**, *371*, 46.